in which m is the total mass of the spacecraft. Whereas matrices J and J_u are positive definite, J_c is only positive. It follows that for any arbitrary vector α, the quadratic forms associated with J and J_u satisfy the inequality

$$\alpha^T J\alpha \leq \alpha^T J_u \alpha \tag{6}$$

Using the theorem of the next section, however, we conclude that

$$\beta^T J^{-1}\beta \geq \beta^T J_u^{-1}\beta \tag{7}$$

Hence, introducing the functional

$$\kappa_I = \tfrac{1}{2}\beta^T J_u^{-1}\beta + V_{EL} \tag{8}$$

and considering inequality, Eq. (7), we can write

$$\kappa \geq \kappa_I \tag{9}$$

so that the system is asymptotically stable if κ_I is positive definite.

The implication of inequality, Eq. (9), is that it is possible to use the testing functional κ_I for stability analysis instead of κ. Because κ_I is free of the terms involving the shifting of C, the stability analysis can be simplified considerably by using κ_I as a testing functional instead of κ. The conclusion is valid irrespective of the magnitude of x_c, y_c, and z_c. Of course, when x_c, y_c, and z_c are large the stability criteria derived by using κ_I as a testing functional instead of κ can be unduly restrictive. In most practical cases, however, x_c, y_c, and z_c are one order of magnitude smaller than the elastic displacements themselves, in which case no accuracy is sacrificed by using κ_I instead of κ.

A Theorem on Inequalities for Quadratic Forms

The simplification of the stability analysis resulting from the use of the testing functional κ_I instead of κ was based on the fact that if matrices J and J_u are such that inequality (6) is satisfied then matrices J^{-1} and J_u^{-1} satisfy inequality (7). Of course, matrices J and J_u do satisfy inequality (6), but it remains for us to prove that inequality (7) follows from inequality (6). Consider the following:

Theorem

Given two $n \times n$ matrices A and B which are symmetric and positive definite over the real number field R. If $x^T Ax \geq x^T Bx$ for any n-vector x over R, then $x^T A^{-1}x \leq x^T B^{-1}x$.

Proof:

Because A is symmetric and positive definite, there is an orthonormal matrix U such that[3]

$$A^{-1/2} = U\lambda^{-1/2}U^T \tag{10}$$

where λ is a diagonal matrix with its elements equal to the eigenvalues of the matrix A. The effect of the operation

$$C = A^{-1/2}BA^{-1/2} \tag{11}$$

is to transform the symmetric and positive definite matrix B into a matrix C which is also symmetric and positive definite, i.e.

$$C^T = (A^{-1/2}BA^{-1/2})^T = A^{-1/2}B^TA^{-1/2} = A^{-1/2}BA^{-1/2} = C \tag{12}$$

Similarly, there exists an orthonormal matrix V such that

$$V^TCV = V^TA^{-1/2}BA^{-1/2}V = \mu \tag{13}$$

where μ is a diagonal matrix.

Introducing the linear transformation

$$p = V^TA^{1/2}x \tag{14}$$

into the inequality $x^TAx \geq x^TBx$, where p is an n-vector, we obtain

$$p^TV^TA^{-1/2}AA^{-1/2}Vp \geq p^TV^TA^{-1/2}BA^{-1/2}Vp \tag{15}$$

which reduces to

$$p^TIp \geq p^T\mu p \tag{16}$$

where I is the identity matrix. Because A and B are positive definite, all the elements of the diagonal matrix μ are positive. It follows from inequality (16) that

$$p^TI^{-1}p \leq p^T\mu^{-1}p \tag{17}$$

Moreover, recalling inequalities (15) and (16), it follows that

$$p^TV^TA^{1/2}A^{-1}A^{1/2}Vp \leq p^TV^TA^{1/2}B^{-1}A^{1/2}Vp \tag{18}$$

Next, let

$$y = A^{1/2}Vp = A^{1/2}VV^TA^{1/2}x = Ax \tag{19}$$

so that inequality (18) reduces to

$$y^TA^{-1}y \leq y^TB^{-1}y \tag{20}$$

Because A is symmetric and positive definite, we can show that A can be regarded as a linear transformation mapping the linear space into itself. This concludes the proof that $x^TA^{-1}x \leq x^TB^{-1}x$.

Conclusions

Considerable simplification of the stability analysis for flexible spacecraft can be achieved by ignoring the shifting of the spacecraft mass center relative to the nominal undeformed position. The resulting stability criteria are conservative compared with those obtained by including the shifting of the mass center, but in most practical cases the loss of accuracy is insignificant. To demonstrate the validity of the analysis, a new theorem on inequalities for quadratic forms is advanced and a proof of the theorem is provided.

References

[1] Meirovitch, L., "A Method for the Liapunov Stability Analysis of Force-Free Dynamical Systems," *AIAA Journal*, Vol. 9, Sept. 1971, pp. 1695-1701.

[2] Meirovitch, L. and Calico, R. A., "Stability of Motion of Force-Free Spinning Satellites with Flexible Appendages," *Journal of Spacecraft and Rockets*, Vol. 9, April 1972, pp. 237-245.

[3] Franklin, J. N., *Matrix Theory*, Prentice-Hall, New York, 1968, p. 106.

Nonequilibrium Nozzle Flow of a Nitrogen-Hydrogen Mixture

B. P. Edwards* and R. J. Stalker†

Australian National University, Canberra, Australia

THE high enthalpy nozzle flow of a nitrogen-hydrogen mixture is of interest from two points of view. First,

Received April 28, 1975; revision received August 1, 1975.

Index categories: Nozzle and Channel Flow; Reactive Flows; Thermochemistry and Chemical Kinetics.

*Honors Undergraduate in Physics.

†Reader in Physics. Member AIAA.

because it appears that entry into the atmosphere of Titan will require hypervelocity flight in mixtures which consist predominantly of nitrogen and hydrogen. Second, because the high recombination rate of dissociated hydrogen suggests that significant "freezing" of the gases in the nozzle may be delayed to relatively high stagnation enthalpies. This would be advantageous for studies of real gas effects in hypervelocity flows, as it would permit model flows which exhibit significant real gas effects, whilst retaining an effectively undissociated freestream. This note reports an investigation of a mixture consisting of 50% N_2—50% H_2. It was undertaken with particular emphasis on the second aspect.

Numerical Analysis

A numerical analysis of the nozzle flow was performed using a Univac 1108 computer, and following the program of Lordi et al.[1] Of the seven species considered, equilibrium calculations showed that NH_2 and NH_3 were not present in sufficient quantities to affect the nozzle flow variables. The reactions considered in the nonequilibrium case are listed in Table 1.

The reactions are written in the direction for which rate data were available. Equilibrium constants are calculated using thermodynamic data from both JANAF tables[7] and NASA SP-3001.[8] The dominant vibrating species were N_2 and H_2, and their vibrational behavior was represented by independent "sudden freeze" approximations. The NH concentration was such that a consideration of its vibration was unnecessary.

The behavior of the nozzle expansion was investigated over a range of stagnation enthalpies. At low enthalpies nitrogen was not dissociated in the nozzle reservoir, and the expansion was dominated by the effects of hydrogen recombination. However, as enthalpies increased, the exchange reactions 8 and 10 played an important role. Reaction 8 produced NH and reaction 10 destroyed it. The net effect of this was to cause recombination of nitrogen, with the atomic hydrogen concentration being held at a high level, despite competition from the fast direct hydrogen recombination.

Results for the flow at the exit of a conical nozzle are shown in Fig. 1. The total included divergence angle of the nozzle was 14°, and the throat diameter was 1.6 mm. It can be seen that hydrogen atoms are expected to constitute the dominant atomic species over the range of enthalpies investigated. H atom concentrations are such that the freestream value of γ, the ratio of specific heats, changes by less than 1% up to stagnation enthalpies of 25MJ/kg.

The quantity $1\text{-}h_f/h_0$ is plotted, where h_f is the freestream frozen enthalpy, and h_0 is the stagnation enthalpy. This quantity is a measure of the efficiency of conversion of stagnation enthalpy into directed kinetic energy at the nozzle exit. Reactions 7 and 9 were found to have little effect on the expansion, and the influence of the exchange reactions 8 and 10 was determined by performing the calculations with only reactions 1-6 included, and plotting the results on the broken curve. Comparison between the two curves demonstrates the effectiveness of the exchange reactions in reducing the frozen enthalpy of the expanded flow.

It may be noted that the rate data for the reactions 8-10 are based on theoretical calculations, performed by Mayer et al.,[9,6,5] using modifications of the Johnston-Parr[10] method for predicting kinetic behavior for hydrogen atom transfer reactions.

Experiments

The experiments were performed in a small free-piston shock tunnel,[11] using a nozzle as specified in the previous section. The exit diameter of the nozzle was 38 mm.

Spark schlieren photographs were taken of the oblique shock formed on a symmetrical two-dimensional wedge, and of the bow shock on a circular cylinder mounted transverse to the stream. The oblique shock measurements were designed to check the value of γ in the freestream, whilst the purpose of the experiments on the cylinder was to observe the effects of postshock reactions in the flow.

For the oblique shock measurements, a wedge was used with an included angle of 70° between the wedge faces. The angle between the shock wave and the wedge face was measured. This angle depended upon the density ratio across the shock wave and, since a strong shock was formed on the wedge, the density ratio depends upon the freestream value of $\gamma\text{-}1$. The variation of shock-wedge angle with time was measured for a number of stagnation enthalpies to confirm that a test period existed during which the shock angle was constant. Results for the value of the shock-wedge angle during the steady period are plotted against stagnation enthalpy in Fig. 2a. The stagnation enthalpy was calculated from measurements of the shock speed, and the pressure after shock reflection in the shock tube.

Theoretical curves also are shown in Fig. 2a. These curves incorporate small corrections, of the order of 1°, for boundary-layer effects on the wedge flow, and for nozzle source flow effects. The corrections were made according to the methods outlined by Stalker and McIntosh[12] for air. Curve (i) shows the expected variation of shock-wedge angle in the absence of chemical or vibrational relaxation. Estimates of vibrational relaxation times were made using the data of Kiefer and Lutz[13] for hydrogen, and Millikan and White[14] for nitrogen. They indicated that hydrogen vibration would equilibrate close to the shock, but nitrogen vibration would remain frozen. Curve (ii) incorporates the effect of hydrogen vibration. It can be seen that the experimental results are in accord with curve (ii), and effectively confirm the expected variation of freestream γ with stagnation enthalpy.

It should be noted that the results in Fig. 2a do not allow differentiation between atomic hydrogen and atomic nitrogen in the freestream, and therefore cannot be used as a means of detecting the effects of the exchange reactions 8 and 10.

The bow shock measurements were conducted with a cylinder which was 19 mm in diameter. Results for the shock stand-off are shown plotted in Fig. 2b. Hornung[15] used the

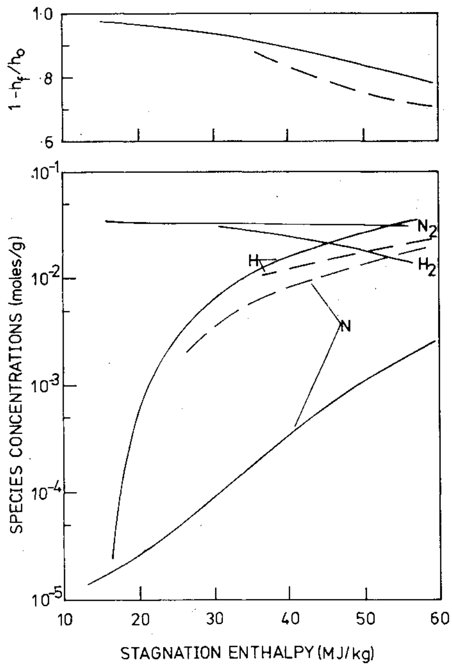

Fig. 1 Properties of expanded flow. ————All reactions in Table 1.---- Reactions 1-6 only. Area ratio = 1000. Stagnation pressure = 200 atm.

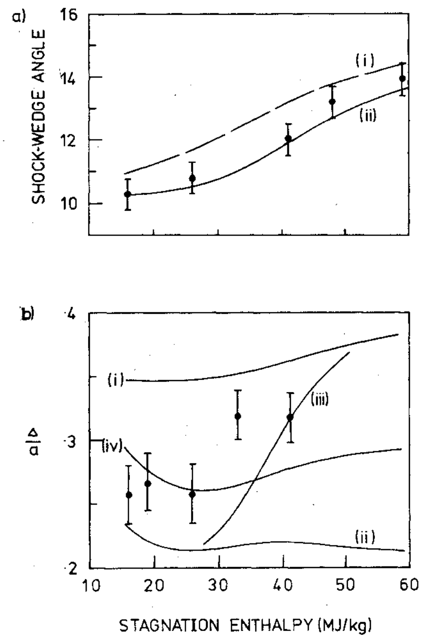

Fig. 2 (a) Shock-wedge angle on wedge. (i) Chemistry and vibration frozen. (ii) H_2 vibration in equilibrium after shock. (b) Shock stand-off on cylinder. Δ = Stand-off; a = Cylinder radius. (i) Frozen chemistry. (ii) Equilibrium after shock. (iii) Hydrogen equilibrium, nitrogen frozen. (iv) Prediction of nonequilibrium calculations. Vibration in equilibrium in all cases.

method of Lomax and Inouye[16] to calculate the bow shock stand-off on a cylinder. He obtained a correlation between shock stand-off and shock density ratio for the case of a non-relaxing gas in the shock layer. Hornung's correlation was combined with appropriate equilibrium shock density ratios to obtain the curves (i), (ii), and (iii) in Fig. 2b. In the case of curve (iv), where the gas was relaxing within the shock layer, the density distribution along a constant pressure streamtube downstream of the shock wave was calculated, using the reaction system of Table 1, and this was used to obtain a mean density in the shock layer. This mean density was then used, in conjunction with Hornung's correlation, to derive a shock stand-off distance.

Two points arise from the experimental results. First, it can be seen that they are consistent with the nonequilibrium calculations at low stagnation enthalpies. The stand-off distances correspond to mean shock layer densities in excess of 8, and confirm that real gas effects are occurring in the shock layer under conditions where Fig. 2a indicates a freestream value of γ close to 1.4. Second, as enthalpies exceed 30 MJ/kg, the measured stand-off distance increases, and the results tend to become consistent with curve (i) or (iii), rather than curve (iv). In the nonequilibrium calculations on which curve (iv) is based, this range of enthalpies corresponded to the region in which dissociation of hydrogen was replaced by dissociation of nitrogen as the dominant cause of density increase in the shock layer. This was the result of an enhanced disssociation rate for nitrogen, arising from reactions 8, 9, and 10. The increase in shock stand-off raises the possibility that the enhancement does not occur, and suggests that it would be worthwhile conducting shock tube experiments to check the theoretical rates used for reactions 8, 9, and 10.

Table 1 Reactions included in the analysis

Reaction	A_i	n_i	E_i(cal-mole^{-1})	Ref.
1. $N_2+N_2 \rightarrow 2N+N_2$	3.7E+21	−1.6	2.25E+05	2
2. $N_2+N \rightarrow 2N+N$	1.6E+22	−1.6	2.25E+05	2
3. $N_2+H,H_2 \rightarrow 2N+H,H_2$	1.9E+17	−0.5	2.25E+05	3
4. $H_2+H_2 \rightarrow 2H+H_2$	3.3E+15	0.0	1.053E+05	4
5. $H_2+H \rightarrow 2H+H$	2.12E+15	0.0	8.72E+04	4
6. $H_2+N,N_2 \rightarrow 2H+N,N_2$	1.0E+21	−1.5	1.031E+05	3
7. $NH+M \rightarrow N+H+M$	6.9E+11	0.5	8.9E+04	3
8. $H+NH \rightarrow H_2+N$	1.0E+12	0.68	1.9E+03	5
9. $2NH \rightarrow N_2+H_2$	3.6E+11	0.55	1.9E+03	3
10. $N+NH \rightarrow N_2+H$	5.0E+11	0.5	2.0E+03	6

where $k_f = A_i T^{n_i} \exp(-E_i/RT)$cm^3 mole^{-1} sec^{-1}

References

[1] Lordi, J. A., Mates, R. E., and Moselle, J. R., "Computer Program for the Numerical Solution of Nonequilibrium Expansions of Reacting Gas Mixtures," CR-472, May 1966. Cornell Aeronautical Lab., Buffalo, N.Y.

[2] Appleton, J. P., Steinberg, M., and Liquornik, D. J., "Shock-Tube Study of Nitrogen Dissociation Using Vacuum-Ultraviolet Light Absorption," *Journal of Chemical Physics*, Vol. 48, Jan. 1968, pp. 599-608.

[3] Prud'homme, R. and Lequoy, C., "Tableau des Vitesses Specifiques de Reactions Chimiques Utilisables en Aerothermochimie," TN 147, March 1969, Office Nationale D'Etudes et de Recherches Aerospatiales, (Chatillon, France).

[4] Breshears, W. D. and Bird, P. F., "Precise Measurements of Diatomic Dissociation Rates in Shock Waves," *14th Symposium on Combustion*, 1972, pp. 211-217.

[5] Mayer, S. W., Schieler, L., and Johnston, H. S., "Computed High-Temperature Rate Constants for Hydrogen-Atom Transfers Involving Light Atoms," *Journal of Chemical Physics*, Vol. 45, July 1966, pp. 385-391.

[6] Tunder, R., Mayer, S., Cook, E., and Schieler, L., "Compilation of Reaction Rate Data for Nonequilibrium Performance and Re-entry Calculation Programs," TR-1001 (9210-02)-1, Jan. 1967, Aerospace Corp., El Segundo, Calif.

[7] Stull, D. R., *JANAF Thermochemical Tables*, Aug. 1965, Dow Chemical Co., Midland, Mich.

[8] McBride, B. J., Heimes, S., Ehlers, J. G., and Gordon, S., "Thermodynamic Properies to 6000 K for 210 Substances Involving the First 18 Elements," NASA Rep. SP-3001, 1963.

[9] Mayer, S. W., Schieler, L., and Johnston, H. S., "Computation of High-Temperature Rate Constants for Biomolecular Reactions of Combustion Products," *11th International Symposium on Combustion*, 1966, Berkeley, Calif., pp. 837-844.

[10] Johnston, H.S. and Parr, C., "Activation Energies from Bond Energies. 1. Hydrogen Transfer Reactions," *American Chemical Society Journal*, Vol. 85, Sept. 1963, pp. 2544-2551.

[11] Stalker, R.J., "A Study of the Free-Piston Shock Tunnel," *AIAA Journal*, Vol. 5, Dec. 1967, pp. 2160-2165.

[12] Stalker, R.J. and McIntosh, M. K., "Hypersonic Nozzle Flow of Air with High Initial Dissociation Levels," *Journal of Fluid Mechanics*, Vol. 58, May 1973, pp. 749-761.

[13] Kiefer, J. H. and Lutz, R. W., "Vibrational Relaxation of Hydrogen," *The Journal of Chemical Phsycis*, Vol. 44, Jan. 1966, pp. 668-672.

[14] Millikan, R. C. and White, D. R., "Vibrational Energy Exchange between N_2 and CO. The Vibrational Relaxation of Nitrogen," *The Journal of Chemical Physics*, Vol. 39, July 1963, pp. 98-101.

[15] Hornung, H. G., "Nonequilibrium Dissociating Nitrogen Flow over Spheres and Circular Cylinders," *Journal of Fluid Mechanics*, Vol. 53, Part 1, May 1972, pp. 149-176.

[16] Lomax, H. and Inouye, M., "Numerical Analysis of Flow Properties about Blunt Bodies Moving at Supersonic Speeds in an Equilibrium Gas," NASA TR R-204, July 1964.